KERNFORSCHUNGSZENTRUM

KARLSRUHE

Dezember 1968

KFK 899
EUR 4166 e

Institut für Neutronenphysik und Reaktortechnik
Institut für Angewandte Reaktorphysik

Experience Obtained at Karlsruhe with Different Kinetic Methods of Reactivity Determination

H. Borgwaldt, M. Edelmann, F.W.A. Habermann, G. Kußmaul,
H. Meister, W. Seifritz, D. Stegemann

GESELLSCHAFT FÜR KERNFORSCHUNG M.B.H.

KARLSRUHE

KERNFORSCHUNGSZENTRUM KARLSRUHE

Dezember 1968

KFK 899
EUR 4166.e

Institut für Neutronenphysik und Reaktortechnik
Institut für Angewandte Reaktorphysik

EXPERIENCE OBTAINED AT KARLSRUHE WITH DIFFERENT KINETIC METHODS OF REACTIVITY DETERMINATION *

H. Borgwaldt, M. Edelmann, F.W.A. Habermann **
G. Kußmaul, H. Meister, W. Seifritz, D. Stegemann

Paper presented to the
PANEL ON REACTIVITY MEASUREMENTS
of the International Atomic Energy Agency
Vienna, 9 - 13 December 1968

* Work performed within the association in the field of fast reactors between the European Atomic Energy Community and Gesellschaft für Kernforschung m.b.H., Karlsruhe.

** EURATOM Delegate.

Contents

1. Introduction

In this survey paper we intend to summarize experience obtained at the Karlsruhe Nuclear Research Center with different methods of reactivity measurement. A common feature of all methods treated here is that they rely on an analysis of the kinetic behaviour of the reactor, utilizing either some external perturbation or the inherent neutron fluctuations.

Whereas in the sections 2 to 4 methods are listed that use the complete set of reactor kinetic equations and involve, primarily, the delayed neutron parameters, the sections 5 to 8 deal with methods utilizing only the prompt-neutron kinetics. In section 9 an aspect common to all kinetic methods is briefly explained, viz. the problem of error estimates and error minimization in experiments on near-critical systems.

Although, generally, the meaning of reactivity is somewhat uncertain, we believe that this is not an important point in simple systems which are not too far from critical. Only such systems are considered in this paper.

Another aspect, which may complicate the interpretation of kinetic experiments in terms of reactivity, is the possible non-separability of the space-energy and the time dependence. In general, we will assume the simplest situation, in which the point-reactor model is valid, but will point out also some cases where contamination by higher modes has been observed. In the sections 3 and 7.2 two experiments on a special reactor configuration are treated, which could be interpreted in terms of a two-node approximation and yielded a coupling reactivity.

All experiments have actually been performed on zero power reactors, i.e. on the Fast-Thermal Argonaut Reactor Karlsruhe (STARK), on a thermal Argonaut configuration (ARK), and on the fast critical SNEAK.

2. Experience with Various Reactivity Measurement Methods at STARK

2.1 Theoretical Model

During the investigation of different fast core loadings of the coupled Fast-Thermal Argonaut Reactor Karlsruhe STARK [1-3] a series of reactivity measurements were performed. To determine larger reactivity worths ($|\rho| \gtrsim 2\ \not{c}$), asymptotic period, rod drop and "inverse kinetics" techniques have been employed. For measurements of central reactivity worths of small samples ($|\rho| \lesssim 2\ \not{c}$) also a square-wave pile-oscillator was used.

Whereas the asymptotic period method poses no problems, the other methods exhibit some features not commonly known, that will be described in the following. In all cases the time behaviour of the neutron population, n(t), was observed and subsequently analyzed. The well-known kinetics equations of a point reactor were consistently used as the theoretical model for all methods of reactivity evaluation. Usually these equations write as follows:

$$\begin{aligned} \frac{dn}{dt} &= \frac{\rho(t)-\beta}{\Lambda}\, n(t) + \sum_{i=1}^{N} \lambda_i\, C_i(t) + S(t) \\ \frac{d\,C_i}{dt} &= \frac{\beta_i}{\Lambda}\, n(t) - \lambda_i\, C_i(t) \qquad (i = 1,\ldots N)\ , \end{aligned} \tag{2.1}$$

where all symbols have the usual meaning.

Some words should be said on $\beta_i = \beta_{i_{eff}}$, the effective fraction of the i^{th} group of delayed neutrons and N, the number of delayed neutron groups. Because of the difference in the λ_i-values for U^{235} and U^{238} [4], 12 delayed neutron groups were used, 6 for each isotope contained in the assemblies. The effective fractions $\beta_{i_{eff}}$ and the generation time of the prompt neutrons, Λ, were derived from a 26-group perturbation calculation:

$$\beta^{M}_{i_{eff}} = \beta_i^{M}\ \frac{\int_V \sum_{j,k} \phi_j^{+} \chi_{ij} \cdot \nu\Sigma^{M}_{fk}\, \phi_k\, dV}{\sum_{M} \int_V \sum_{j,k} \phi_j^{+} \chi_j \cdot \nu\Sigma^{M}_{fk}\, \phi_k\, dV} \tag{2.1a}$$

$$\Lambda = \frac{\int_V \left(\sum_k \phi_k^+ \frac{1}{v_k} \phi_k \right) dV}{\sum_M \int_V \left(\sum_{j,k} \phi_j^+ \chi_j \nu \Sigma_{fk}^M \phi_k \right) dV} , \qquad (2.1b)$$

where β_i^M = actual fraction of the i^{th} delayed neutron group of isotope M and χ_{ij} = energy distribution of the i^{th} delayed neutron group, energy group j, and all other symbols have the usual meaning of multigroup formalism. In order to obtain the energy distributions χ_{ij}, the measured spectra of delayed neutrons [5] were adapted to the group division of the 26-group-ABN-set [6].

2.2 Experimental Setup

The coupled zero-power reactor STARK consists of a subcritical fast core (containing a mixture of platelets of U_{nat}, 20% enriched U, and nonfissile materials) driven by a surrounding light-water moderated annular thermal zone with 20% enriched U-fuel (cf. Fig.1). 12 cadmium-plate control units are evenly distributed around the thermal core, and an additional fuel-poison safety rod (S_4) is installed in the fast core.

The neutrons are detected by a B^{10}- or He^3-ionization chamber normally located near the thermal core in the graphite reflector. The chamber signal is amplified by an electrometer amplifier and then fed to a voltage-to-frequency converter, the output of which consists of a pulse train with a frequency proportional to the input signal. These pulses are counted in a 256-channel multiscaler time analyzer.

2.3 The Inverse Kinetics Method

The eq.(2.1) can be converted into the following integro-differential-equation

$$\frac{\rho(t)}{\beta} + \frac{\Lambda \cdot S(t)}{\beta \cdot n(t)} = 1 + \frac{1}{n(t)} \left[\frac{\Lambda}{\beta} \frac{dn}{dt} - \sum_{i=1}^{N} a_i e^{-\lambda_i t} \left(n_o + \lambda_i \int_o^t n(\tau) e^{\lambda_i \tau} d\tau \right) \right] , \qquad (2.2)$$

where $a_i = \beta_i/\beta$. In a source-free system ($S(t) \equiv 0$) or at a power level where the source term is negligible, the measured signal n(t) can be converted by means of eq.(2.2) into the reactivity of the system starting from the stationary and critical value n_o. A FORTRAN programme is used to calculate the right-hand side of eq.(2.2).

This method, often called "inverse kinetics" method, was widely used in our investigations. If a control or safety rod is inserted with constant velocity, the reactivity vs. position-characteristics can be determined in a single run. The applicability ranges from minute reactivity values (cf. section 2.5) to very large values of some $. Our investigations showed [7] that this method is also very useful in the evaluation of rod drop measurements, if some precautions are observed (cf. section 2.4).

2.4 Rod Drop Method

For a source-free point-reactor, the neutron signal after a step change of reactivity applied at $t = 0$ to a stationary and critical system ($n(t) = n_o$, for $t < 0$) is given by

$$\frac{n(t)}{n_o} = \sum_{j=o}^{N} A_j \, e^{s_j t} , \qquad (2.3)$$

where s_j are the N+1 roots of the inhour equation

$$s\left(\Lambda + \sum_{i=1}^{N} \frac{\beta_i}{s+\lambda_i}\right) - \rho = 0 \qquad (2.4)$$

and

$$A_j = \frac{1 + \frac{1}{\Lambda} \sum_{i=1}^{N} \frac{\beta_i}{s_j+\lambda_i}}{1 + \frac{1}{\Lambda} \sum_{i=1}^{N} \frac{\lambda_i \beta_i}{(s_j+\lambda_i)^2}} \qquad (j = 0,\ldots N) .$$

A detailed analysis of the experimental $n(t)/n_o$-curves revealed a strong variation in the amplitude of the prompt transient with detector position (cf. Fig.1), whereas a few seconds after completion of the reactivity change a common space-independent time behaviour was observed [7]. To eliminate spatial effects from the experimental data, n(t) was normalized not to the initial value n_o but rather to a value n(T) some seconds after

the drop ($T \gtrsim 5$ sec) which is not influenced by higher spatial modes of the prompt neutron distribution. The reactivity values ρ/β were obtained by comparison of the experimental ratios $n(t)/n(T)$, for $t > T$, with those calculated by eq.(2.3), $\Sigma A_j e^{s_j t} / \Sigma A_j e^{s_j T}$, and were found to be independent of detector position within $\pm$ 2 percent (cf. column 3 of Table 1).

Compared to the space-independent model, the prompt transient is larger for detector positions close to the control plate and smaller for positions far away. On the boundary of both regions, appropriate detector positions exist (at an azimuthal angle of $\approx 60^{o}$ from the plate), where n(t) was found to agree well with the space-independent calculation in its entire time-behaviour. In these positions complete control plate characteristics were determined by the inverse kinetics method and no systematic deviations from the other methods were observed.

Fig.1 clearly shows that all evaluation methods which utilize the initial value n_o must fail unless an appropriate detector position is chosen (cf. column 4 of Table 1).

2.5 Pile-Oscillator Measurements

Measurements of reactivity worths of small material samples ($|\rho| \lesssim 2\ ¢$) in the central channel of the fast zone have been carried out with a pile-oscillator. A square stainless steel tube was filled with 4.6 cm x 4.6 cm platelets of core material to an overall height of 120 cm (core height 60.5 cm, upper and lower blanket 8.4 cm each). Two aluminium containers, one for the sample and the other empty were embedded in the oscillator rod at two positions, 21.3 cm each from the rod center. The oscillator rod was connected to the piston of a driving mechanism actuated by compressed air. The stroke of the oscillator was 42.5 cm so that the sample could be moved from the center of the core to a position outside the blanket. The transient time between both positions was $\approx$1 sec such that the reactivity approximately changed in a square-wave manner with a period T = 64 sec.

A large part of the B^{10}-ionization chamber signal was suppressed while the oscillating part was recorded, as described in section 1, by a 256-channel time analyzer which was synchronized with the oscillator in such a manner that two consecutive periods were stored in each analyzer sweep. Normally 10 double-periods were sampled to improve the signal/noise ratio. The mean reactor power was 10 watts; small reactivity drifts during the experiment were compensated by a slowly moving fine-control rod.

The experimental data were analyzed on a IBM-7074 digital computer in two ways. The first method was a Fourier analysis and the second an evaluation by the inverse kinetics programme described in section 2.3.

If a reactor is considered as a linear system, the input and output signals can be decomposed into sine-waves of frequency $k\omega$, where $\omega = 2\pi/T$ is the fundamental frequency of the input. Theoretical considerations lead to the following expression between the Fourier amplitude C_k of the neutron signal and the reactivity amplitude Δ of a square-wave

$$\frac{C_k}{n_o} = \begin{cases} \frac{4}{\pi k} |\Delta| \cdot |G(jk\omega)| & (k=1,3,5,\ldots) \\ 0 & (k=2,4,6,\ldots) \end{cases} , \tag{2.5}$$

where

$$G(jk\omega) = \frac{1}{jk\omega \left[\Lambda + \sum_{i=1}^{N} \frac{\beta_i}{jk\omega + \lambda_i} \right]} \tag{2.6}$$

is the (calculated) reactor transfer function.

In an ideal square-wave oscillation only odd harmonics are present. In the actual experiment, however, also even modes are excited by reactor noise and neutron scattering effects during the sample motion. A strong additional component of twice the fundamental frequency is observed, which is caused by the periodical removal and reinsertion of irradiated fuel containing delayed neutron precursors.

The Fourier analysis of the experimental data which encompasses an even number of periods stored as a two-period train, as described above, was accomplished in five steps. Starting with the data comprising the first period ($0 \leq t \leq T$), the analysis is shifted by T/4 in each step ($T/4 \leq t \leq 5T/4$, $T/2 \leq t \leq 3T/2$ etc.). The calculated sine- and cosine-coefficients are combined in such a manner as to eliminate the drift components up to second order within the measuring interval. Table 2 contains the reduced amplitudes C_k/n_o and the resulting reactivity values up to the seventh mode together with the drift-corrected values for a sample of 36.56 grams of 93.15 % enriched uranium and for a sample of 0.356 grams of boron (92.15 % enriched in B^{10}) in an aluminium container of 32.8 grams.

The second reactivity evaluation makes use of the inverse kinetics programme. The data, to which the constant suppressed signal is added, are analyzed by this programme. One difficulty arises in so far as eq.(2.2) uses the initial value n_o corresponding to a critical and stationary system, while our experimental data start from an asymptotic oscillating state. This difficulty is overcome by applying eq.(2.2) to data obtained from a periodical continuation of the measured two-period train. The resulting reactivity $\rho(t)$ converges against the asymptotic signal after 4 to 5 continuations (about 10 min), since the initial value n_o is successively suppressed by the weighting factors $e^{-\lambda_i t}$ in eq.(2.2).

Fig.2 shows the reactivity values obtained by the above procedure for the uranium-sample. These values are considered to consist of two parts. The first part is the value of the material sample ρ_M/β, which is constant but of different sign within each half-period. The second time-dependent part can be interpreted as a (negative) source term, $\Lambda S(t) / \beta\, n(t)$, which describes the net withdrawal of precursors out of the system. Theoretical considerations based on the point-reactor model [8] lead in a first approximation to the following expression for the fictitious source

$$S(\tau) = -\gamma \frac{n_o}{\Lambda} \sum_{i=1}^{N} \beta_{i\,eff} \frac{1-e^{-\lambda_i \frac{T}{2}}}{1-e^{-\lambda_i T}} e^{-\lambda_i \tau} \qquad (0 \leq \tau \leq \frac{T}{2}). \qquad (2.7)$$

γ is the net fraction of precursors withdrawn from the reactor. In a first approximation $S(\tau)$ is periodical with frequency 2ω . The difference of corresponding reactivity values of two successive half-periods therefore yields the value ρ_M/β of the sample. These values are shown in Fig.3. The mean value for the first and second period of the data are included in Table 2. Fig.3 also shows a set of reactivity values which have been calculated in the same way but with the delayed neutron parameters of U^{235} (thermal fission) given by KEEPIN [4] instead of the effective parameters described in section 2.1. Whereas the reactivity values obtained with the effective data set are fairly constant, the values obtained with the KEEPIN-set indicate a time-dependence.

3. Kinetics and Reactivity Determination in a System of Two Loosely Coupled Cores

The kinetic behaviour of a system composed of two loosely coupled cores can be treated by coupled kinetics equations [9-12]. These equations are derived from the kinetics equations of two point reactors by substituting the external sources by coupling terms which describe the neutron exchange between the two core zones. Because the main emphasis was laid on rod drop measurements, the time-behaviour is predominantly determined by the delayed neutron precursors and the neutron transition time between the core zones can be neglected [13]. In this case the coupling term from zone y to zone x writes

$$S(t)_{y \longrightarrow x} = \frac{\varepsilon_{yx}}{\Lambda} n_y(t) \ , \qquad (3.1)$$

where ε_{yx} = coupling coefficient for neutron exchange from y to x,
$n_y(t)$ = neutron population in zone y.

Under the further assumption of equal prompt neutron generation times and precursor parameters (β_i, λ_i) the kinetics equations are solved in the case of step reactivity perturbations applied at t = 0 to the critical system.

A detailed derivation is given in [14]. The roots of the resulting "inhour equation" are there shown to split into two sets, each of which satisfies an inhour equation of a one-point reactor. This leads to two parameters ρ_1 and ρ_2; ρ_1 being the reactivity of the entire system and ρ_2 characterizing the change in the spatial distribution of the neutron populations. The time-behaviour of the core x is given by

$$\frac{n_x(t)}{n_{xo}} = \frac{(n_y/n_x)_o + (n_x/n_y)_\infty \varepsilon_{xy}/\varepsilon_{yx}}{(n_y/n_x)_\infty + (n_x/n_y)_\infty \varepsilon_{xy}/\varepsilon_{yx}} P(\rho_1,t) + \frac{(n_y/n_x)_\infty - (n_y/n_x)_o}{(n_y/n_x)_\infty + (n_x/n_y)_\infty \varepsilon_{xy}/\varepsilon_{yx}} P(\rho_2,t), \tag{3.2}$$

where $(n_x/n_y)_o$ is the initial ratio and $(n_x/n_y)_\infty$ is the asymptotic ratio of the neutron populations. These ratios and $\varepsilon_{xy}/\varepsilon_{yx}$ are measurable quantities. The function $P(\rho_j,t)$ describes precisely the response of a point reactor to a step change ρ_j in reactivity starting from critical as given by eq.(2.3). Thus, eq.(3.2) expresses the time behaviour of each separate core as a sum of two terms describing point reactors. The term $P(\rho_2,t)$ in eq.(3.2) contributes only when $(n_x/n_y)_\infty \neq (n_x/n_y)_o$, i.e. if the spatial distribution of the population changes with time. From eq.(3.2) for each core we get

$$P(\rho_1,t) = \frac{n_x(t)/n_{xo}}{1 + (n_y/n_x)_o (n_y/n_x)_\infty \varepsilon_{yx}/\varepsilon_{xy}} + \frac{n_y(t)/n_{yo}}{1 + (n_x/n_y)_o (n_x/n_y)_\infty \varepsilon_{xy}/\varepsilon_{yx}} . \tag{3.3}$$

This equation and the corresponding expression for $P(\rho_2,t)$ suggest a method to weight the time behaviour of the individual zones x and y, to isolate the terms $P(\rho_j,t)$. As these functions describe point reactors, they can be analyzed by the known methods of point reactor kinetics.

A series of measurements were performed at the so-called two-slab loading of the Argonaut-Reactor Karlsruhe (ARK), which has been obtained by substituting the fast core of the STARK-reactor by a graphit column. The fuel elements are arranged inside of the annular tank in two groups of 131 fuel plates each. The detectors are placed in the outer reflector behind each zone.

Step changes of reactivity were produced by dropping one or several control plates. To evaluate the time behaviour, the inverse kinetics programme (cf. section 2.3) was used. The results obtained showed that the two-point reactor model is very useful to describe the time behaviour of a system of two loosely coupled cores and that reactivity measurements can be performed with methods known from the point reactor. For the coupling reactivity $\varepsilon_{xy}/\beta = \varepsilon_{yx}/\beta$ this method gave 3.08 $ in good agreement with another method treated in section 7.2.

4. Experience with Various Reactivity Measurement Methods at SNEAK

In the course of two years of operation a number of reactivity measurement methods have been utilized [16,17] at the fast zero power facility SNEAK [15]. The methods have been adapted and extended to comply with the special requirement for high precision measurements being carried out with a minimum of reactor time. Lately the inverse kinetics method has been almost exclusively used, both for control rod calibrations and for the measurement of small sample worths; other methods proved to be not as versatile. A description of special features added to various methods is given together with a discussion of the experience gained since SNEAK went into operation in December 1966.

4.1 Equipment

Three linear flux measuring channels are installed for experimental purposes. As detectors three large BF_3-chambers are positioned in various locations at the outer edge of the reactor blanket of depleted uranium. The locations are chosen in such a way that spatial effects during control rod calibrations can be minimized. The ionchambers are surrounded with polyethylene plates in order to raise their sensitivity to a high enough value that the detection noise in the chamber is smaller than the fluctuations caused by reactor noise. In this way the theoretical precision limit of measured reactivity that can be reached at a certain reactor power within a certain length of time is approached closely. Two types of amplifiers have been utilized. The amplifier type, which is now

preferred for SNEAK experiments because of its favourable characteristics, uses voltage dependent capacitors in its input. Zero drift is negligible, and the overall linearity was measured to be within 0.03 %.

In order to allow digital treatment of the flux data the output voltages of the amplifiers are digitized by voltage to frequency converters with a maximum frequency of 10^5 pulses/sec. The output pulses of these ADC's are counted during a certain time interval. The contents of the counters have up till now been punched on paper tape before further digital analysis was performed off-line. The information had to be punched on cards before a computation could run on an IBM 7074. At the end of 1967 a DDP 124 computer was purchased for use in the experiment control room. The vicinity of this computer and its ability to use punched paper tape as input has reduced the time that elapses between a measurement and its analysis to some hours. It has been experienced in several cases that this period is still too long to allow repetition of a measurement of which the results were not satisfactory. Optimum use of reactor time can only be achieved by fully on-line data treatment. In order to arrive at this an interface is being built between the experiment electronics and the computer. The DDP 124 has a 16 K core memory, 1.75 µsec cycle time, and is equipped with fixed wired floating point arithmetics. This allows on-line calculation and plotting of reactivity with a digital plotter even with the extended version of inverse kinetics calculation of reactivity that is described briefly below.

4.2 Asymptotic Period Measurements

This method was extended to allow measurements at low power in assemblies with a large intrinsic neutron source, which is the case in a Pu-reactor [18]. After transients have died out, the neutron population n(t) in a reactor with a neutron source of strength S behaves as

$$\ln\left(n(t) + \frac{l\,S}{k-1}\right) = t/T + C\ , \qquad (4.1)$$

where l = the neutron lifetime,
$k-1$ = the excess multiplication,
T = the asymptotic period, and
C = a constant.

The magnitude of the source term that makes $\ln(n(t) + 1 S/(k-1))$ satisfy the linear relationship (4.1) is found by an iterative procedure on a digital computer. Using the error propagation law, the uncertainty in both the asymptotic period and the source term are calculated by the code. As disadvantages inherent to the asymptotic period method remain:

(a) It is difficult to eliminate the influence of reactor drift.

(b) An asymptotic period is established only after transients have died out.

(c) If the period is relatively short, the reactor power level has to be brought back after each measurement.

(d) For safety reasons the maximum positive reactivity that can be covered with one measurement is very limited (this makes e.g. control rod calibrations very time consuming).

(e) The asymptotic period is not a sensitive indication for large negative reactivity steps.

A series of small sample reactivity measurements was made in such a way that (c), (d), and (e) did not occur [17]. The reactivity variations were made small enough to prevent large power fluctuations, so that it was not necessary to interrupt reactor operation. The reactor periods were generally larger than 1000 sec; flux data were collected during 10 min for each sample. A precision of $\pm$ 0.002 ¢ was achieved when the reactor drift was small. With a reactor drift of .02 ¢ per hour the error came close to $\pm$ .01 ¢, which is considered too large for small sample reactivites, especially when sample worths in various surroundings have to be compared or selfshielding effects are studied.

4.3 Fourier Analysis of a Periodic Signal

In contrast to the previous method one can collect data continually during an arbitrary length of time with the oscillating method and the influence of reactor drift can be effectively eliminated. At SNEAK the influence of linear drift is removed by a digital program that cross-correlates the experimental signal with a cosine. This is made possible by storing consecutive periods of the signal in a multichannel analyzer in such a way that the initial phase can be varied over 1/4 period. By

addition of counts in a multichannel analyzer one achieves a substantial data reduction, but counting errors in individual periods and nonlinearity of drift are masked. At SNEAK a sample travels more than 15 sec from its "in" position to its "out" position in the horizontal sample drawer. Due to this it was not possible to rule out the influence of the transients on the first harmonic of the flux oscillations to the extreme accuracy that was desired for the sample measurements. Since under these circumstances an error calculation becomes problematic, the method is not used at SNEAK any more.

4.4 Autorod

A high precision automatic rod has been built which accurately compensates reactor perturbations and measures their magnitude in terms of rod travel. The rod is moved automatically until the output of a linear channel equals a highly stabilized reference voltage. The time constant of the rod is smaller than 0.1 sec, and its digital position indication system has a resolution of one part in 10^5. With these characteristics reactor noise is reflected in movements of the rod, and high precision reactivity measurements are possible. The data treatment is simple because the characteristic of the rod is practically linear. Since, however, the worth of the rod depends on the assembly in which it is used and on its location it has to be recalibrated whenever changes occur.

4.5 Reactivity Meter /19/

This instrument is a small 10 volt transistorized analog computer with a fixed wired program for solving the inverse kinetics equations. The signal of an ionization chamber channel serves as on-line input. The output is a continuous reactivity information, which is displayed on a recorder in the control desk and on one in the experiment control room. Six ranges from 0.5 ¢ up to 5 $ full scale can be chosen. In the most sensitive range reactivity can be read off with an accuracy of $\pm$ 0.02 ¢ at a reactor power of 30 watts. An input signal smaller than 5 % of full scale does not allow accurate computation of reactivity any more. Six chopper stabilized operational amplifiers and one servomultiplier are the active elements of the meter. The time constants of six delayed neutron terms

are taken into account by R-C-combinations. The neutron source term simulator is changed automatically to another value when the range of the ionization chamber amplifier is switched.

The reactivity meter has proven to be an extremely useful instrument for reactivity measurements with moderate precision and for easy operation of the reactor. The operator can adjust the reactor to criticality very simply, and the experimenter has immediate information on reactivity changes, also transients, that occur (Fig.4). In some cases no other reactivitiy determination than with the reactivity meter was needed, e.g. when the reproducibility of the reactor after various manipulations was tested. During other reactivity measurements the meter is used as a display unit only: The reactivity track on the recorder is not suited for further treatment, such as calculation of average reactivities and standard deviations.

4.6 Inverse Kinetics, Digital

The utilisation of the inverse kinetics method offers for oscillating measurements over Fourier analysis the advantage that each data point is treated separately, so that false counts (e.g. zero) can easily be detected and, secondly, that a drift correction can be made separately for each period. Transients, e.g. when a sample traverses the reactor core, are treated correctly by the program and do not influence the computed reactivities of the "in" and the "out" position. A whole series of samples can be measured without interruption if they can be exchanged without shutting the reactor down. The SNEAK horizontal sample drawer is equipped with a sample changer that takes 25 samples. The whole sequence of inserting, withdrawing and exchanging samples can be performed automatically by a program on punched paper tape.

Several extensions have been made to the program that solves the inverse kinetic equations. A routine to determine the magnitude of an intrinsic neutron source in the reactor was incorporated in the first place /20/. It starts with solving eq.(2.2) for a negative reactivity step. The left hand side ρ' of this equation consists of a constant reactivity and a flux dependent source term. The slope of ρ' vs. $1/n(t)$ gives the source term. As long as the neutron source is a constant this term can be used in consecutive calculations of reactivity.

It is necessary to fill the sample drawer with core material in the vicinity of the sample if one does not want to perturb the spectrum there. In order to avoid large reactivity transients during sample traverses the drawer should be filled completely with the same material. Not only fissionable material, but also the delayed neutron precursors that have been built up in it are moved with the drawer to locations with different importance. This effect is not treated by the point kinetic equations; they have therefore been extended in such a way that this effect is taken into account. The point kinetic equations can be used for the description of a multizone reactor if one gives the variables effective values which are composed of the variables of separate reactor zones by weighting them with the adjoint fluxes in these zones. Condition for the applicability of extended point kinetics is that the fission rate distribution remains constant, which is the case when a homogeneous drawer moves. In a zone where fuel moves the change of the precursor concentration is given by production minus decay plus net transport

$$\frac{dC_i}{dt} = \beta_i \, k(t) \, \frac{n(t)}{l} - (v \, C_i(t,\vec{r}), \, \vec{v}(t,\vec{r})) - \lambda_i C_i(t,\vec{r}) \, , \qquad (4.2)$$

in which $\vec{v}$ = the velocity of the fuel, $\vec{r}$ = position.

This is taken into account for the channel through which the sample drawer moves in the KINEMAT code [21]. The channel is divided in a number of zones, and the precursor concentrations are calculated for each counting interval. With this computation the initial drift of the reactivity steps that is shown in Fig.2 disappears.

It is now meaningful to calculate the standard deviation of each step in order to determine the influence of reactor statistics. Large differences in standard deviations of consecutive steps are an indication of gross deviations in count rates, e.g. caused by electronic failures or punching faults. The occurance of false count rates is serious, since they influence the reactivity computation at later times. In order to eliminate such faults an optional routine has been added to the programme that eliminates those count rates that deviate more than two times the standard deviation from the five previous values or do not lie either below the maximum or above the minimum of 5 following countrates. A countrate that is considered

as false by these criteria is replaced by the average of the previous and the following values. This routine can only be applied when no reactivity peaks of short duration occur. Optionally the computer program can plot all reactivity values with a digital plotter.

All measured sample worths are corrected for linear reactor drift by averaging the reference positions before and after the "sample-in" position. The actual drift of the "sample-out" reference positions is also tested for linearity, and nonlinear drift contributions are taken into account as additional terms in the error calculation. This KINEMAT code /21/ is now in routine use and works to our complete satisfaction. As an example of this evaluation a sample reactivity measurement is shown in Fig.5.

5. Rossi-Alpha Experiments

In a reactor with a constant fission rate F the expected number of counts from a neutron detector of sensitivity W (counts/fission) during an arbitrary time interval ΔT is $WF\Delta T$. If one considers an observation interval of length ΔT which starts at a time $(T-\Delta T/2)$ after an arbitrary initiating (or triggering) pulse from a first detector (sensitivity W_1), the expected number of counts from a second detector (sensitivity W_2) is given by /22/

$$E(T) = W_2(F + A\, e^{-\alpha T})\ \Delta T\ , \qquad (5.1)$$

assuming $T > \Delta T/2$ and $\alpha\Delta T \ll 1$. The increased detection probability (5.1) is due to the possibility of detecting several, correlated neutrons of the same prompt neutron chain.

According to eq.(5.1), measuring the time distribution of pulses from the second detector, following an a r b i t r a r y triggering pulse from the first detector allows, primarily, the determination of the prompt neutron decay constant α. It is related to the reactivity ρ/β through

$$\rho/\beta = 1 - \alpha\Lambda/\beta\ . \qquad (5.2)$$

All methods of reactivity measurement, which use this expression to convert measured decay constants α into reactivities, depend on the α-value at delayed critical, $\alpha_c = \beta/\Lambda$, which must be known. Especially in fast reactors, α_c is difficult to compute. Some methods, e.g. noise analysis experiments, may determine α_c directly. For Rossi-alpha and also for pulsed neutron experiments, this is difficult to perform. In these cases we choose to correlate measured α-values with independently measured average detector count rates, which are inversely proportional to reactivity, and obtain α_c by extrapolation to delayed critical.

When, as one usually assumes in theory, all pulses of the first detector can serve as trigger pulses for the time analyzer, the constand A in (5.1) is

$$A = C_1 \frac{\overline{\nu(\nu-1)}_p}{2\,\bar{\nu}^2} \frac{k^2\,\alpha}{(1-k(1-\beta))^2} \approx C_1 \frac{0.4\,k^2\,\alpha}{(1-k(1-\beta))^2} \quad . \tag{5.3}$$

Herein k = effective multiplication constant and C_1 is a geometry dependent normalization factor of order unity /23/. In this case the total count rate for pairs of detector pulses separated in time by $(T \pm \Delta T/2)$ becomes

$$R_o(T)\,\Delta T = W_1\,W_2\,F\,\Delta T(F + A\,e^{-\alpha T}) \quad . \tag{5.4}$$

It is very important to exploit fully this possible rate of delayed coincidences and keep all losses in the analyzing equipment negligibly small. In references /24/ and /25/ the theory of dead time losses in the trigger channel of a Rossi-alpha experiment has been developed to some extent. With a dead time τ in the channel of the trigger detector we obtain instead of (5.4) an expression

$$R(T)\,\Delta T = \gamma_1 W_1 W_2\,F\,\Delta T(F + \gamma_2\,A\,e^{-\alpha T}) \quad . \tag{5.5}$$

If the dead time τ is short, one may expand the correction factors γ_1, γ_2 in powers of τ ,

$$\gamma_1 = 1 - W_1(F + A)\tau \quad + - \ldots \tag{5.6a}$$

$$\gamma_2 = 1 - W_1(F + A)\tau \quad + - \ldots \quad . \tag{5.6b}$$

In the most conventional type of Rossi-alpha experiment pulses from the trigger detector are used to start an analyzing cycle of a multichannel time analyzer, which registers subsequent pulses from the same or a second detector until the analyzing cycle is completed /26/. No new trigger pulse is accepted before the end of the cycle. Thus, the dead time τ in the trigger channel is equal to the cycle time T_c of the analyzer.

Assuming that (a) $\alpha\, T_c \gg 1$ and (b) the time analyzer accepts during one cycle time T_c any number of pulses from the second detector subsequent to the trigger pulse, we get an expansion in powers of W_1 /24/

$$\gamma_2 = 1-(F+A)\, W_1/\alpha + 1/2(F^2 + 5\, FA + 4\, A^2)(W_1/\alpha)^2 \qquad (5.7)$$
$$- \ldots$$

For the special case of a very low fission rate, $F \ll A$, this becomes /24/:

$$\gamma_2 = \frac{2}{1 + \sqrt{1 + 4\, A\, W_1/\alpha}} \,. \qquad (5.7a)$$

Dead time losses obviously reduce the cycle frequency of the time analyzer, cf. equations (5.5), (5.6a). The approximations (5.6b), (5.7), (5.7a) for the factor γ_2, valid under different limiting conditions, all show that the signal/background ratio (γ_2 A/F) is adversely affected. Both effects strongly reduce the counting rate (5.5) of delayed coincidences and tend to increase severely the statistical errors in the determination of α. They are emphasized by high sensitivities W_1 of the trigger detector, by high fission rates F and in near-critical systems. Finally, there is some evidence, that such Rossi-alpha experiments performed under unfavourable conditions may not be free from systematic errors. With low signal/background ratios the evaluated decay constants α seem to come out systematically too small /25/.

In order to overcome these difficulties different modifications of the Rossi-alpha technique have been proposed and investigated /24,25/. The simplest way to reduce dead time effects in the trigger channel connected to a conventional multichannel time analyzer is the reduction of the pulse rate of the trigger detector. This can be done (a) by using, only in the trigger channel, a detector with a lower sensitivity W_1 or (b) in a more flexible manner by chopping the signal of the trigger detector. The preferred technique consists in gating the trigger input of the time analyzer periodically

by a square wave pulse generator with a variable period T_1 and pulse width T_o so that detector pulses can initiate time analyzer cycles only within the periodic time intervals T_o spaced by intervals (T_1-T_o), which should be larger than the cycle time T_c of the analyzer. It has been demonstrated that the loss factor γ_2 increases with decreasing gate width T_o and approaches unity for $T_o \rightarrow 0$. Evidently a decrease of T_o also decreases the effective trigger pulse rate by the factor

$$\gamma_1 \approx T_o/T_1 \quad . \tag{5.8}$$

Therefore, a value of T_o has to be chosen, which yields optimum performance. It has been found, that in cases of low signal/background ratios A/F T_o should be chosen according to

$$W_1 \, F \, T_o \lesssim 0.2 \tag{5.9}$$

to achieve reasonable results. Under these conditions Rossi-alpha experiments on STARK loading 2 (with β/Λ = 70/sec) could be performed in the reactivity range from 0.3 to 4.2 $ subcritical, with signal/background ratios from 0.07 to 0.32, using a TMC Multichannel Analyzer with Pulsed Neutron Plug-in Model 212. In the available time only limited accuracy was achieved, but without the gating technique no results at all could be obtained /25/.

A modification of this technique applies additional scaling down of the pulses from the first detector so that in each of the periodic gate intervals of length T_o only the n-th arriving pulse can trigger the time analyzer (n = 2 to 4, and T_o larger than given by eq.(5.9)). Although in the experiments on STARK the theoretically predicted increase in the signal/background ratio could be verified, the overall performance of this modification was not encouraging /25/.

A problem of the described gating technique is the required time for a measurement, which can become prohibitively long, when the fission rate F and the trigger detector pulse rate are very high and the signal/background ratio, accordingly, becomes low. An efficient off-line method of reducing the dead time effects of the analyzer, practically to zero, has been found in the use of magnetic tape recorders /25/.

In this technique the pulses from the neutron detectors and a periodic trigger gate pulse generator (pulse width T_o, period T_1) are simultaneously recorded on different tracks of the magnetic tape. These records are repeatedly analyzed with a gated time analyzer as described before. During the successive playbacks of these records the gate signal is delayed in steps of T_o until all pulses of the trigger detector have once been brought to coincidence with a gate pulse. The number of playbacks needed is obviously T_1/T_o.

In this way, with sufficiently short gate pulses, nearly all pulses of the first detector can be utilized for once triggering the time analyzer. This method simulates off-line the ideal Rossi-alpha experiment without dead time losses. In principle, it is equivalent to the first method using a periodically gated time analyzer but reduces the necessary reactor operating time by the factor T_o/T_1.

For the reduction of dead time effects in on-line Rossi-alpha measurements a new time analyzer /25/ has been developed, in which the dead time between two successively starting time cycles is only one channel width instead of one cycle length in conventional analyzers. It consits of a 132-stage digital shift register (manufactured by Borer und Co., Solothurn, Switzerland) which controls a number of 32 coincidence channels and is, in principle, a very versatile digital version of the delayed coincidence analyzer described by ORNDOFF /22/. In ORNDOFF's analyzer the trigger detector pulses were delayed by delay lines from which they were fed into coincidence counting channels. In our new analyzer the trigger detector pulses are digitally delayed by being shifted through the shift register in steps of a variable clock pulse period. One time channel is formed by a sequence of stages of the shift register (selectable by a switch) together with a coincidence circuit and a fast scaler. The channel width can be chosen between 250 nsec and 0.4 sec.

For improving the time resolution of fast transients in the prompt-neutron decay the possibility of using shorter channel widths in the channels 1 to 9 and larger widths in the rest of the time cycle has been incorporated.

This analyzer has been successfully used for Rossi-alpha measurements on STARK loadings 2 and 4 and on the SNEAK assemblies 1 and 3A-2 in the reactivity range of 0.1 to 5 $ subcritical. In 1 hour reactor runs α-values were obtained with errors of about 3 to 5 per cent and in good agreement with pulsed neutron experiments. The α-values range from 60/sec to 90000/sec, and the lowest signal/background ratio A/F, in an experiment on STARK, loading 4, was about 0.01.

It should be noted that some of these measurements have been performed under such extremely unfavourable conditions that even with this new analyzer the previously described technique of gating the trigger input or the recording/playback method had to be used to further reduce or avoid dead time effects.

6. Pulsed Neutron Experiments

At Karlsruhe pulsed neutron experiments have been routinely performed on all STARK loadings in the reactivity range from delayed critical to - 5 $. Pulsed neutron experiments on the SNEAK configurations 1, 3A-0, 3A-1, 3A-3 have been evaluated between a few ¢ subcritical and - 1.5 $. The applied techniques have been explained previously [17,27] in sufficient detail and will not be repeated here.

It is noteworthy that the observed discrepancies between the "stable period $" (measured by the methods of section 4) and the "pulsed neutron $" (obtained by extrapolating pulsed neutron experiments to α = 0) are fairly small in these SNEAK experiments. Maximum deviations are about 10 percent, and it is impossible at the present stage to decide whether these discrepancies are a serious phenomenon or must be attributed to errors in the control rod calibration [28].

7. Noise Analysis in the Frequency Domain

Noise analysis experiments in the frequency domain are performed both on-line and off-line. For the off-line technique tape recording and analysis by a dual channel wave analyzer (Weston Boonshaft and Fuchs, Model 711-CL) is the adopted procedure. This technique allows both the measurement of autopower and crosspower spectral densities and is routinely applied. In the following, two special applications of noise analysis in the frequency domain shall be treated.

7.1 On-Line Reactivity Meter

Reactivity determinations using a two-detector crosscorrelation technique have been realized on-line with a reactivity meter [29-32]. Two crosspower spectral densities $(CPSD)_L$ and $(CPSD)_H$ are measured simultaneously at two frequencies $\lambda_i \ll \omega_L \ll \alpha$ and $\omega_H \gg \alpha$, where α is the break frequency of the crosspower spectrum (= prompt neutron decay constant) and λ_i are the precursor decay constants.

In the point reactor model the reactivity of the system is

$$\frac{\rho}{\beta} = 1 - \frac{\omega_H}{\alpha_c} \sqrt{\frac{(CPSD)_H}{(CPSD)_L}} \qquad (7.1)$$

with $\alpha_c = \beta/\Lambda$. The reactivity meter is designed as an analog computer programmed to compute the expression (7.1) in three steps, whose time succession is controlled by digital logic. The reactivity ρ/β is displayed on a digital voltmeter.

The advantage of measuring crosspower spectral densities, viz. that the output signal of the crosscorrelator contains no uncorrelated noise contribution to the spectral density function, is fully exploited.

Shutdown reactivity measurements have been performed on the Argonaut reactor ARK (cf. section 3), on STARK loading 5 and on the Siemens Training Reactor SUR 100. In all three reactors a strong neutron source (5 C Am-Be; $1.2\ 10^7$ neutrons/sec) was inserted into the core to raise the power level in the lower subcritical states.

The measured reactivities of the reactors ARK and STARK with different control and safety rod positions are given in Table 3. Whereas at STARK the whole range of reactivities down to maximum shutdown was covered, only two reactivity values were measured at ARK, primarily with the aim of comparing measured and calculated error margins.

Shutdown reactivities in the SUR 100 measurements (Table 3) were produced by successively separating the core halves.

The meter is calibrated for zero reactivity at delayed critical, i.e. by α_c-determination. The measured reactivities agree with corresponding values from rod drop measurements within the error margins.

Special attention was given to a comparison of measured and predicted relative statistical precision. Practical formulae, developed in the references [30,33,34], to predict the standard deviation of shutdown reactivity values determined by this reactivity meter, have been satisfactorily verified.

There is some prospect of making shutdown reactivity measurements even in "dirty" power reactors, using current type neutron detectors optimized for minimum gamma sensitivity [35]. As shown in reference [32], the lowest value for the detector sensitivity W, which limits the applicability of the reactivity meter in power reactors, is

$$W_{min} = 1.5 \cdot 10^{-5} \, (0.5 + \phi_\gamma/\phi_n) \, \frac{\text{pulses}}{\text{fission}} \quad , \qquad (7.2)$$

where ϕ_γ is the gamma flux in R/hr and ϕ_n is the neutron flux in n/(cm^{2}sec) at the detector positions. It seems that the necessary high ratio of neutron flux to gamma flux exists in reactors with high intrinsic neutron sources, such as the Pu^{240} inventory of Pu-fuelled fast breeders.

7.2 Determination of the Coupling Reactivity in a Two-Node Symmetrical System

We have applied noise techniques to determine parameters characterizing the degree of coupling in a two-node symmetrical zero power reactor [36-38]. It is advantageous to introduce a new quantity, the Coupled Core Coherence Function $R(\omega)$. It is defined as the cross spectrum of the signals of neutron detectors situated in the two core regions of a two-node system normalized to the geometrical mean of the correlated parts of the two auto-power spectra of the detector signals.

The coherence function thus defined has the advantage of depending only on the coupling between the regions, which are sampled by the detectors, whereas the cross spectral density function itself depends more on the individual characteristics of the regions. The Coupled Core Coherence Function de-emphasizes the fundamental mode influence and emphasizes spatial effects.

In the case of a critical symmetrical two-node system the reactivity of each isolated node $(\rho/\beta)_{node}$ is compensated by the (symmetrical) coupling reactivity, ε/β, and we get either

$$\left(\frac{\rho}{\beta}\right)_{node} = -\frac{\varepsilon}{\beta} = \frac{1}{2}\left[1 - \sqrt{\frac{1 + R_{crit}(\omega_o)}{1 - R_{crit}(\omega_o)}}\right] \text{ or} \qquad (7.3a)$$

$$\left(\frac{\rho}{\beta}\right)_{node} = -\frac{\varepsilon}{\beta} = \frac{1}{2}\left[1 - \sqrt{1 + 2R_{crit}(\omega_o)\left(\frac{\alpha_{coh}}{\alpha_c}\right)^2}\right], \qquad (7.3b)$$

where $R_{crit}(\omega_o)$ is the (asymptotic) value of the coherence function $R_{crit}(\omega)$ on the plateau $\lambda_i \ll \omega_o \ll \alpha_{coh}$. α_{coh} and α_c are the characteristic break frequencies or the half power points of the coherence function and the cross-power spectral density of the critical reactor, respectively.

In the case of weak coupling ($\varepsilon/\beta < 1$ \$) the application of eq.(7.3a), which uses only the low frequency value of $R(\omega)$, gives more accurate estimates of the coupling reactivity ε/β. In the case of strong coupling ($\varepsilon/\beta > 1$ \$) it is better to apply eq.(7.3b), which makes use of other dynamic information available in the measurement.

In the two-slab configuration of the ARK reactor, briefly explained in section 3, the coherence function has been measured and analyzed according to eq. (7.3b), yielding a coupling reactivity $\varepsilon/\beta = 3.07\ \$$ in good agreement with the method of section 3.

Evidently a symmetrical coupled system can be made subcritical either (a) by changing symmetrically the nodal reactivities $(\rho/\beta)_{node}$ or (b) by changing the coupling reactivity (ε/β). In practical situations mixtures of both effects will always be met. Calculations performed in reference [36] for the two extreme cases (a) and (b), but easily generalized to other situations, demonstrate that the coupled core coherence function $R(\omega)$ is a valuable tool to determine the mechanism, by which shutdown reactivity is produced.

8. Digital Noise Analysis by Measurement of Probability Distributions

The method described in this section is based on the direct determination of probability distributions. Its theory as well as its experimental set-up is given in detail in references [39,40]. The method investigates the probabilities $p_n(T)$, that n detection processes occur in a fixed time interval of length T. A classical example is the POISSONian distribution. Its distribution law is valid for completely uncorrelated events. The existence of correlated events leads to probability distributions which deviate from POISSON's law. This deviation is the stronger the higher the degree of correlation. From this deviation reactor parameters, like the prompt neutron decay constant, reactivity etc. can be inferred.

To evaluate measured probability distributions two possibilities exist:

(a) The evaluation of complete probability distributions or of parts of it. This procedure has been followed in references [41,42].

(b) The evaluation of a quantity closely related to the variance over mean ratio. The equation used for this in the point reactor model approximation is given by

$$\frac{\sum_{n=2}^{\infty} p_n(T)\ n(n-1) - \left[\sum_{n=1}^{\infty} p_n(T)\ n\right]^2}{\sum_{n=1}^{\infty} p_n(T)\ n} = \frac{2\ WA}{\alpha}\left[1 - \frac{1 - e^{-\alpha T}}{\alpha\ T}\right], \qquad (8.1)$$

where p_n, n, and T have been explained, W = detector sensitivity, α = prompt decay constant, and A = parameter defined in eq.(5.3).

The special features of the direct determination of probabilities are: (a) the fast and relatively easy collection of data and (b) an advantageous evaluation process of the results in the way shown by eq.(8.1). Advantageous, because here the uncorrelated background (POISSANian contribution) has been suppressed adequately, similar to the procedure in the two-detector crosscorrelation experiments in the frequency domain.

In order to measure the $p_n(T)$ a special fast probability distribution analyzer has been built of which a detailed description is given in reference /39/ together with the complete data acquisition and reduction system. The analyzer consists essentially of a fast acting electronic step switch, which proceeds by one step for each incoming pulse. The combination with a time marker, terminating the length T of the time interval to be investigated, allows a simple and direct determination of the $p_n(T)$.

Experiments have been performed in thermal and fast reactor systems in order to derive the prompt neutron decay constant α, the reactivity ρ/β, and the absolute reactor power. A typical result obtained at the reactor STARK is shown in Fig.6. A fitting procedure to eq.(8.1) was used to derive the prompt neutron decay constant α, which has been plotted versus the reciprocal detector counting rate (upper scale on abscissa). The prompt neutron decay constant at delayed critical, α_c, was determined by this, and the reactivity ρ/β could then be derived using eq.(5.2).

Special attention was given to the positioning of detectors, as indicated in Fig.6, in order to suppress as far as possible nodal contamination by connecting a number of distributed detectors in parallel. In the course of the experiments performed with either one detector in various of the positions indicated in Fig.6 or two detectors connected in parallel (not shown in Fig.6) the presence of nodal contamination was found. In this respect the method is fairly sensitive so that adequate precautions have to be taken, in particular, in complex systems like STARK.

The application of this technique to fast systems in SNEAK showed the occurrence of strong dead time effects due to high values of α and relatively high counting rates.

Regarding the conclusions for future work to be done for this technique in order to improve reliability, particularly for application in fast systems, it can be stated from the results obtained:

(a) The influence of dead time effects should be eliminated either by a proper theoretical treatment similar to that performed for the Rossi-alpha method or by use of faster electronics.

(b) A detailed theoretical treatment of error estimation similar to the direction followed for the frequency analysis of noise is needed.

9. Reevaluation of Error Estimates

In many methods of reactivity measurement, e.g. pulsed neutron and Rossi-alpha experiments, the primary quantities, which have to be converted into reactivities (cf. eq.(5.2)), are the prompt decay constant of the neutron population, amplitudes, phase shifts, etc. Often the least square fit technique is used to derive these parameters from the experimental data. It yields estimates both of these parameters and their probable errors.

The least square fit technique is strictly applicable only when there is no correlation in the errors of the experimental data. It can be shown, however, that in experiments with sensitive detectors on near-critical assemblies this condition is not met. This correlation of errors appears to be, in practice, more important than is generally recognized.

Primarily, only the probable errors determined by least square fitting become significantly too low, when the parameter

$$y \approx 0.4\, W / (1 - k_p)^2 \qquad (9.1)$$

is comparable to unity (W = detector sensitivity, $k_p = k(1-\beta)$ = prompt multiplication factor). As the simplest model case we may consider a pulsed neutron experiment, in which the pulses have been very widely spaced so that the expected behaviour of the neutron population is simply

$$n(t) = A \cdot e^{-\alpha t} . \qquad (9.2)$$

One may in this case determine an estimate for the decay constant α from experimental data by least square fitting. Then the true probable error of this α-value becomes larger by a factor $\sqrt{1 + 4y}$ than the probable error determined by the least square fit technique /43/. This means that the estimated error of the associated reactivity according to eq.(5.2) can be quite wrong.

In addition, for rather high, but practically attainable values of y also the parameters estimated by least square fitting can have systematic errors, because for obtaining the estimate a wrong procedure was chosen.

In reference /43/ some more cases of general interest are to be treated. But much more work is necessary in order to get for all types of reactor kinetics experiments more reliable estimates of the associated errors and improved estimating procedures, which take error correlation into account.

For experiments with reactivity modulation general error estimates have been derived as well as criteria for the optimization of such pile oscillator experiments /43/. According to these theoretical investigations it is advantageous

(a) to use square wave modulation,

(b) to use adequate filtering for noise rejection,

(c) to have high detector sensitivities,

(d) to derive from the detector used for the experiment also the signal (if any) that generates reactivity feedback for compensating drift.

The last feature (d) minimizes noise in the very important low frequency region. Autorod experiments appear to meet all these conditions most easily. One interesting result was that the minimum error obtained theoretically under optimum conditions is identical with the value given by BENNETT and LONG for their autorod experiment /44/.

References

/1/ BARLEON, L. et al.: Evaluation of Reactor Physics Experiments on the Coupled Fast-Thermal Argonaut Reactor STARK. KFK-482 and ANL-7320, 1966.

/2/ BARLEON, L. et al. (compiled by H. MEISTER): Untersuchungen an der Ladung 2 des Schnell-Thermischen Argonaut-Reaktors STARK. KFK-592, 1967.

/3/ BARLEON, L. et al. (compiled by G. KUSSMAUL and H. MEISTER): Untersuchungen an den Ladungen 3 und 4 des Schnell-Thermischen Argonaut-Reaktors STARK. KFK-668, 1967.

/4/ KEEPIN, G.R.: Physics of Nuclear Kinetics. Addison-Wesley Publishing Company, Inc., Reading, Ma., 1965.

/5/ BATCHELOR, R. and H.R. McHYDER: J. Nucl. Energy 3, 7 (1956).

/6/ ABAGJAN, L.P., N.O. BAZAZJANC, I.I. BONDARENKO, and M.N. NIKOLAEV: Gruppenkonstanten schneller und intermediärer Neutronen für die Berechnung von Kernreaktoren. KFK-tr-144, 1964.

/7/ KUSSMAUL, G.: Unpublished.

/8/ KUSSMAUL, G. and H. MEISTER: To be published.

/9/ BALDWIN, G.C.: Nucl. Sci. Eng. 6, 320 (1959).

/10/ SCHWEIZER, G. and R. LAUBER: Atomkernenergie 6, 242 (1961).

/11/ DANOFSKY, R.A. and R.E. UHRIG: Nucl. Sci. Eng. 15, 131 (1963).

/12/ SEALE, R.L.: Coupled Core Reactors. LAMS-2967, 1964.

/13/ KOEHLER, W.H. et al.: Fast Reactor Physics, Vol.I, 529, IAEA, Vienna, 1968.

/14/ KUSSMAUL, G.: Theoretische und experimentelle Untersuchungen zum Zweipunktreaktor. Externer Bericht INR-4/68-17, Kernforschungszentrum Karlsruhe, 1968.
KUSSMAUL, G.: Zeitverhalten und Reaktivität schwach gekoppelter Spaltzonen. Nukleonik (in press).
BORGWALDT, H., H. KUESTERS, G. KUSSMAUL, H. MEISTER, and K. THURNAY: Reactor Dynamics Topics Recently Investigated at Karlsruhe. KFK-786 and EUR 3958.e, 1968.

/15/ ENGELMANN, P. et al.: Construction and Experimental Equipment of the Karlsruhe Fast Critical Facility, SNEAK. KFK-471, 1966.

/16/ ENGELMANN, P. et al.: Operational Characteristics and Related Design Features of SNEAK. Fast Reactor Physics, Vol.II, 35, IAEA, Vienna, 1968, and KFK 632, EUR 3676.e, 1967.

/17/ STEGEMANN, D. et al.: Physics Investigations of a 670 l Steam Cooled Fast Reactor System in SNEAK, Assembly 3A-1. Fast Reactor Physics, Vol.II, 79, IAEA, Vienna, 1968, and KFK-627, EUR 3671.e, 1967.

/18/ HABERMANN, F.W.A. and H. WALZE: Nucl. Sci. Eng. 33, 262 (1968).

/19/ WALZE, H.: Aufbau und Betriebsweise des SNEAK-Reaktivitätsmeters. KFK-739, 1968, and EUR 3722.d.

/20/ CARPENTER, S.G.: Nucl. Sci. Eng. 21, 429 (1965).

/21/ OOSTERKAMP, W.J.: Private communication, 1967.

/22/ ORNDOFF, J.D.: Nucl. Sci. Eng. 2, 450 (1957).

/23/ OTSUKA, M. and T. IIJIMA: Nukleonik 7, 488 (1965).

/24/ BORGWALDT, H.: Einheitliche Theorie der Korrelationsexperimente in Nulleistungsreaktoren. Externer Bericht INR-4/66-5, Kernforschungszentrum Karlsruhe, 1966.

/25/ EDELMANN, M.: Neue Methoden zur Rossi-α-Messung. Externer Bericht INR-4/68-15, Kernforschungszentrum Karlsruhe, 1968.

/26/ BRUNSON, G.S., R.N. CURRAN, J.M. GASIDLO, and R.J. HUBER: A Survey of Prompt-Neutron Lifetimes in Fast Critical Systems. ANL-6681, 1963.

/27/ EDELMANN, M. et al.: Pulsed Source and Noise Measurements on the STARK Reactor at Karlsruhe. Pulsed Neutron Research, Vol.II, 799, IAEA, Vienna, and KFK-303, 1965.
BOEHME, R. et al.: Comparison of Measurements in SNEAK-1 and ZPR III-41. Fast Reactor Physics, Vol.II, 55, IAEA, Vienna, 1968, and KFK-626, 1967.

/28/ BOEHNEL, K. and F.W.A. HABERMANN: Private communication, 1968.

/29/ SEIFRITZ, W. and D. STEGEMANN: Transactions Am. Nucl. Soc. 10, No.1, 283 (1967).

/30/ SEIFRITZ, W. and D. STEGEMANN: Nukleonik 9, 169 (1967).

/31/ SEIFRITZ, W. and D. STEGEMANN: Transactions Am. Nucl. Soc. 11, No.2, 565 (1968).

/32/ SEIFRITZ, W. and D. STEGEMANN: An On-Line Reactivity Meter Based on Reactor Noise Using Two-Detector Crosscorrelation. Nucl. Applications (in press).

/33/ SEIFRITZ, W., D. STEGEMANN, and W. VAETH: Two-Detector Cross Correlation Experiments in the Fast-Thermal Argonaut Reactor STARK. Neutron Noise, Waves, and Pulse Propagation, 195, AEC Symp. Ser. No.9, Oak Ridge, Tenn., 1967, and KFK-413, 1966.

/34/ SEIFRITZ, W. and D. STEGEMANN: Nukleonik 10, 158 (1967).

/35/ ROUX, D.P.: Nucl. Applications 3, 575 (1967).

/36/ ALBRECHT, R.W. and W. SEIFRITZ: Nukleonik 11, 143 (1968).

/37/ SEIFRITZ, W. and R.W. ALBRECHT: Nukleonik 11, 149 (1968).

/38/ ALBRECHT, R.W. and W. SEIFRITZ: The Coherence Function: A Measure of Spatially Dependent Nuclear Reactor Properties. Proc. Japan/U.S. Seminar on Reactor Noise Analysis, Tokio, Sept. 1968.

/39/ STEGEMANN, D.: Bestimmung reaktorphysikalischer Parameter aus dem Reaktorrauschen durch Analyse von Wahrscheinlichkeitsverteilungen. KFK-542, 1967.

/40/ BORGWALDT, H. and D. STEGEMANN: Nukleonik 7, 313 (1965).

/41/ ZOLOTUKHIN, V.G. and A.I. MOGILNER: Atomnaya Energiya 15, 11 (1963).

/42/ TÜRKCAN, E. and J.B. DRAGT: Fast Reactor Physics, Vol.I, 467, IAEA, Vienna, 1968.

/43/ BORGWALDT, H.: Error Estimates for Kinetic Experiments in Zero Power Reactors. To be published.

/44/ BENNETT, E.F. and R.L. LONG: Nucl. Sci. and Eng. 17, 425 (1963).

Detector position	Control plate or safety rod	ϱ/β evaluated by normalization to n(10)	ϱ/β evaluated from $n(10)/n_o$
A_1	R_1	- 33.0 ¢	- 35.6 ¢
A_2		- 32.9	- 37.0
A_3		- 32.5	- 33.7
A_4		- 32.9	- 32.2
B_1		- 33.0	- 35.6
A_1	R_2	- 28.0 ¢	- 27.2 ¢
A_2		- 27.8	- 27.4
A_3		- 27.8	- 27.2
A_4		- 28.1	- 65.5
B_1		- 27.9	- 27.4
A_1	S_3^2	- 30.8 ¢	- 50.7 ¢
A_2		- 30.8	- 62.5
A_3		- 30.6	- 33.2
A_4		- 30.7	- 29.8
B_1		- 30.8	- 62.5
A_1	S_4	- 1.43 $	- 1.43 $
A_2		- 1.41	- 1.45
A_4		- 1.43	- 1.42
B_1		- 1.43	- 1.44

Tab.1 Comparison of reactivity values of three control plates R_1, R_2, and S_3^2, and the safety rod S_4 of STARK measured in different detector positions and evaluated by normalization to $n(10) = n(t = 10\ sec)$ and to n_o. The measured data $n(t)/n_o$ of S_3^2 are shown in Fig.1.

Harmonics index k	Uranium sample (36.56 g U; 93.15 W/o U^{235})			Boron sample (32.8 g Al + 0.356 g B; 92.15 W/o B^{10})		
	C_k / n_o $[10^{-3}]$	$\rho = 2\Delta$ $[10^{-3}\ \$]$	$\rho = 2\Delta$ $[10^{-5}]$	C_k / n_o $[10^{-4}]$	$\rho = 2\Delta$ $[10^{-3}\ \$]$	$\rho = 2\Delta$ $[10^{-5}]$
1	14.37	9.840	7.278	28.81	- 1.972	- 1.459
2	1.116	-	-	11.87	-	-
3	3.082	9.768	7.225	5.965	- 1.891	- 1.398
4	0.6325	-	-	7.404	-	-
5	1.628	9.874	7.303	2.984	- 1.810	- 1.339
6	0.4498	-	-	5.955	-	-
7	1.099	9.955	7.363	2.068	- 1.873	- 1.385
1 drift corrected	14.34	9.815	7.259	28.83	- 1.974	- 1.460
from inverse kinetics	1^{st} period $(9.870 \pm 0.017) \cdot 10^{-3}\ \$$			$(- 1.966 \pm 0.019) \cdot 10^{-3}\ \$$		
	2^{nd} period $(9.758 \pm 0.017) \cdot 10^{-3}\ \$$			$(- 1.972 \pm 0.018) \cdot 10^{-3}\ \$$		

Tab.2 Results of Fourier analysis and inverse kinetics evaluations of pile oscillator measurements of a 93.1 % enriched Uranium and a Boron sample.

ARK $-\rho/\beta$	STARK $-\rho/\beta$	SUR 100 $-\rho/\beta$
(70 ± 5.6) ¢	(42 ± 2) ¢	(50 ± 7) ¢
(1.2 ± 0.1) $	(81 ± 6) ¢	(1.61 ± 0.1) $
	(1.67 ± 0.11) $	(2.13 ± 0.1) $
	(2.54 ± 0.14) $	(2.66 ± 0.12) $
	(3.5 ± 0.12) $	(3.57 ± 0.4) $
	(4.3 ± 0.23) $	5.5 $
		6.1 $
		7 $

Tab.3 Results of shutdown reactivity measurements performed with the on-line reactivity meter of sect.7.1 (time for each measurement = 10 min).

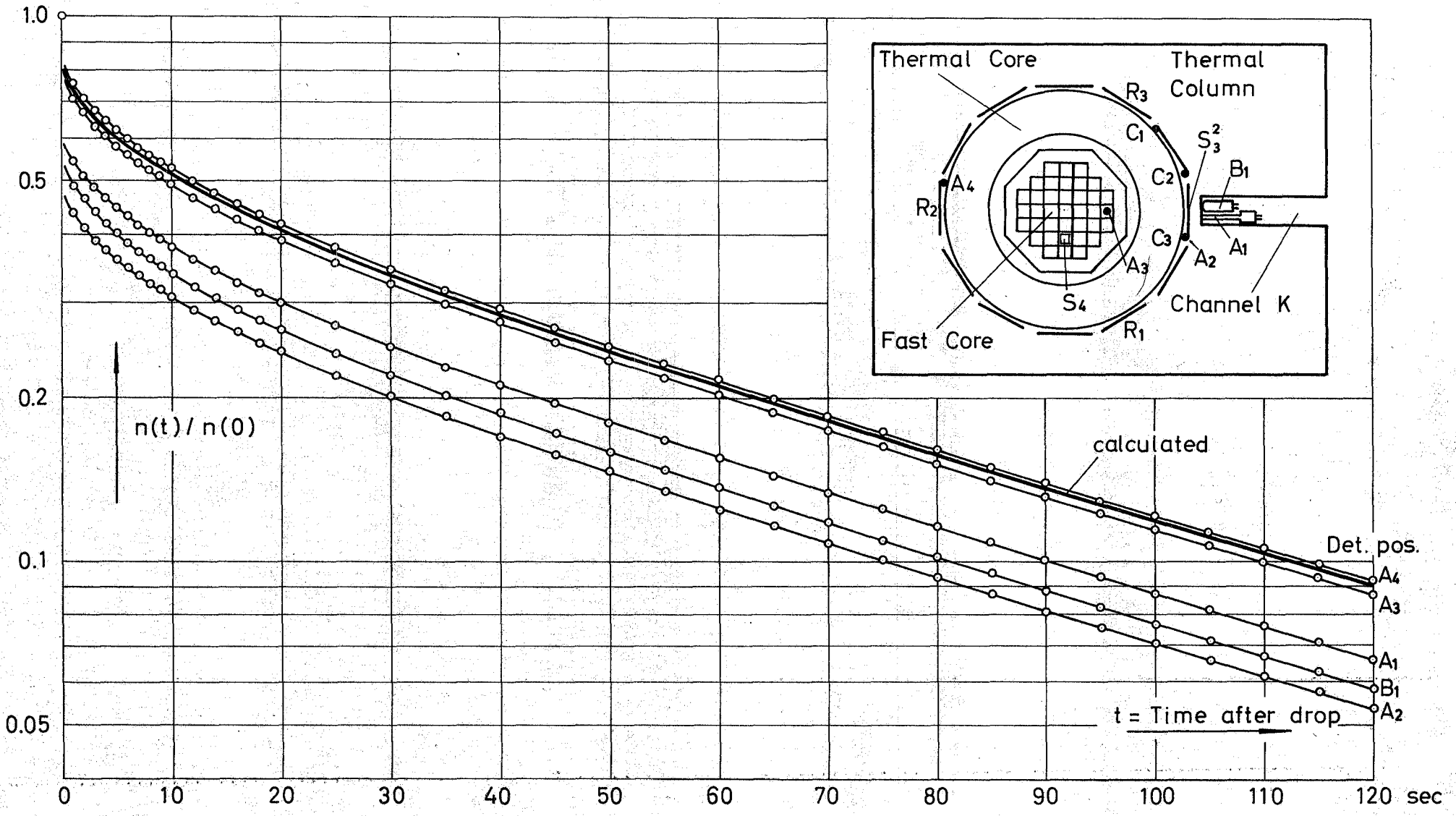

Fig.1 Time behaviour of detector signal in different positions ($A_1,...A_4,B_1$), determined after a rod drop of the control plate S_3^2 of the STARK-Reactor. Schematic cross section of STARK with control plates and detector positions.

——o—— measured

——— calculated by eq.(2.3) for $\rho/\beta = -0.308$ $

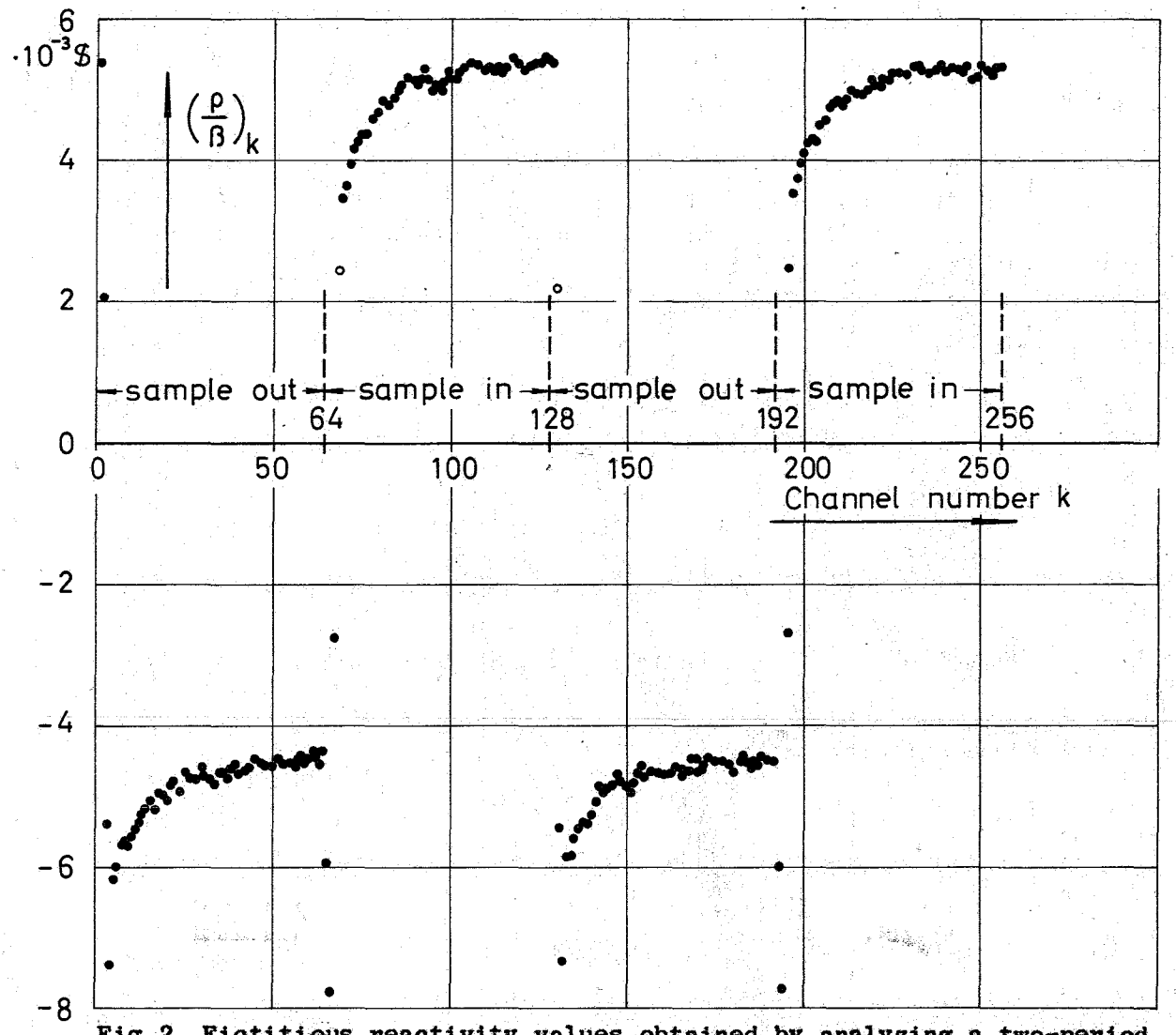

Fig.2 Fictitious reactivity values obtained by analyzing a two-period signal of a pile-oscillator measurement of 93.1 % enriched U-sample with the inverse kinetics programme. Channel width 0.5 sec.

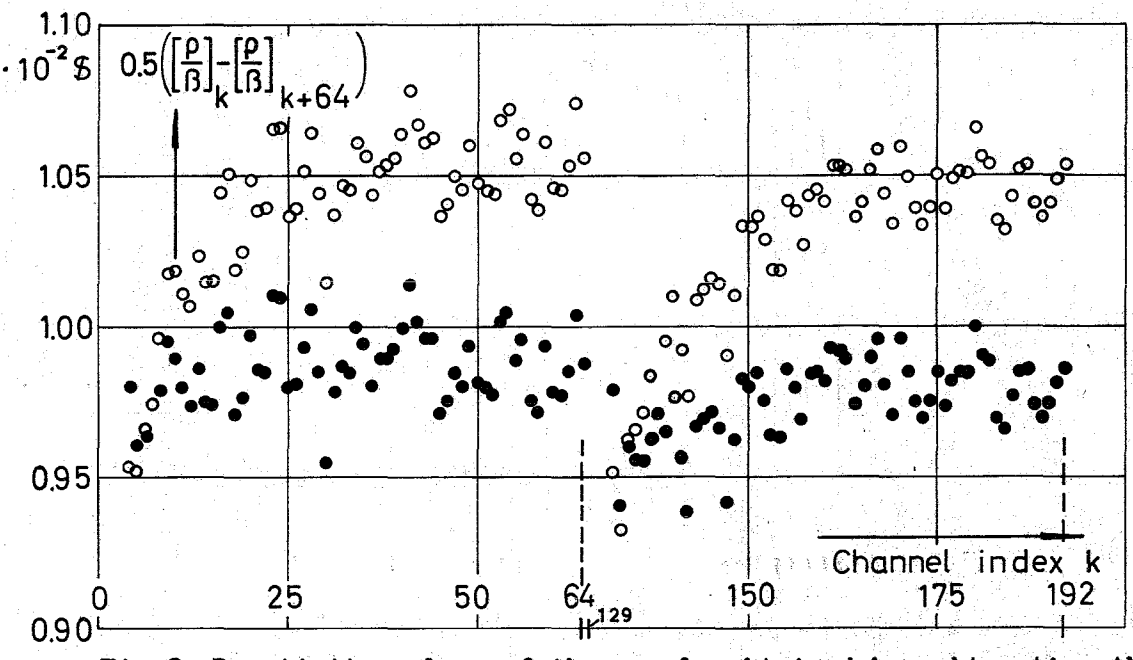

Fig.3 Reactivity values of the sample obtained by subtracting the data of Fig.2 of two consecutive half-periods.

- ● effective 12-group delayed neutron parameter set
- ○ 6-group U^{235}-thermal fission parameter set

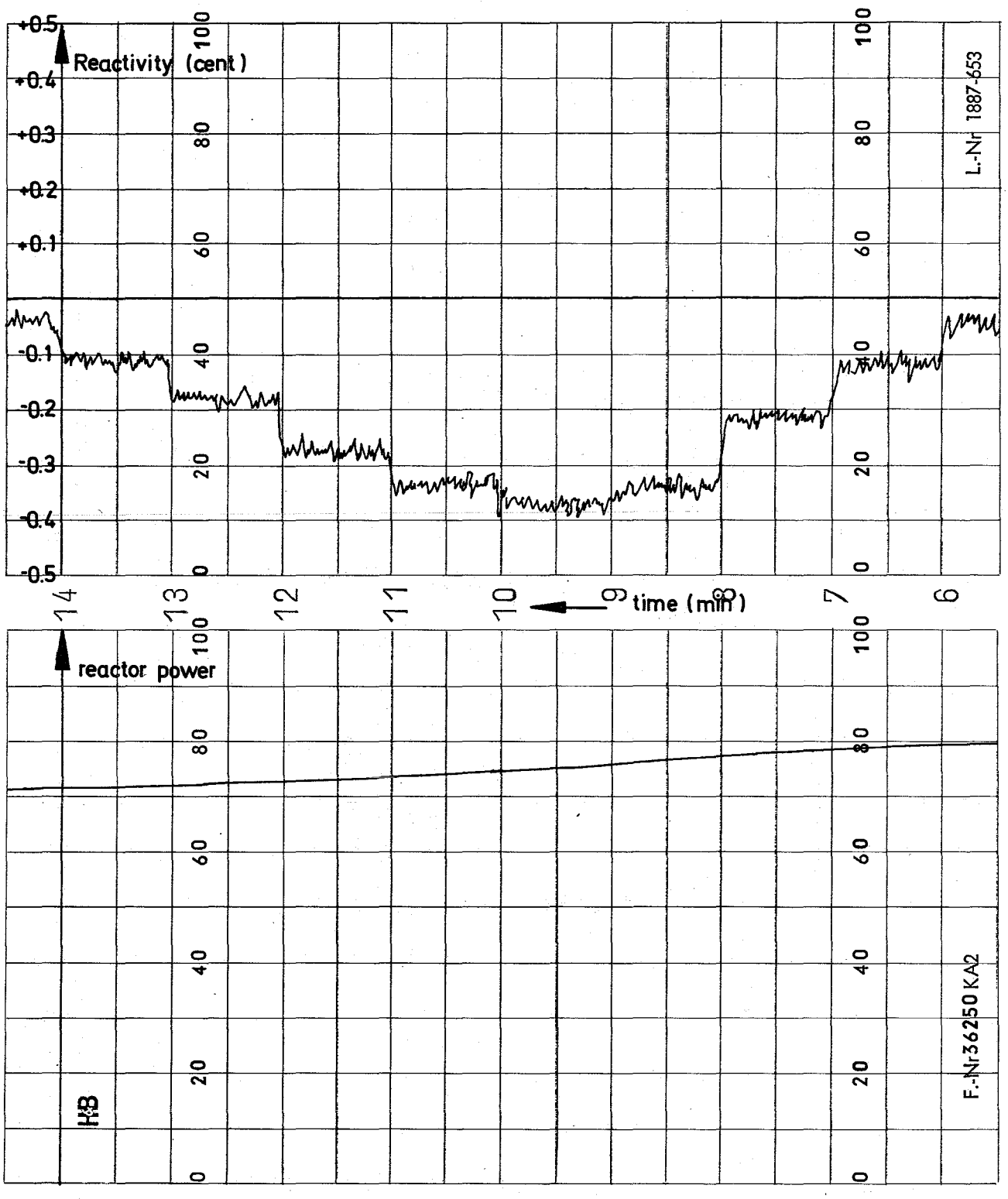

Fig.4 Reactivity traverse of an Al-sample in SNEAK-1 as calculated by the reactivity meter from the time dependent reactor power

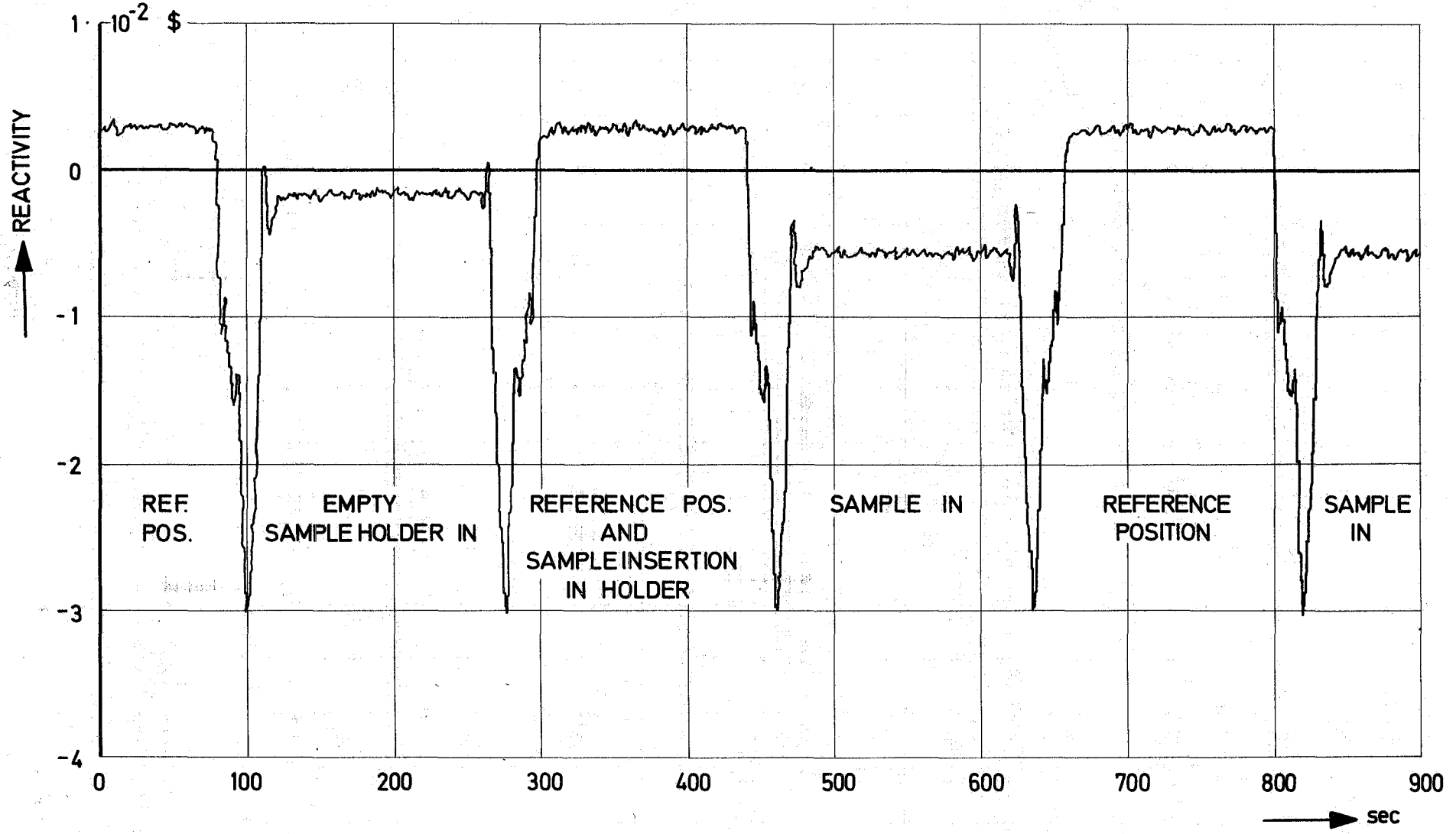

Fig.5 Reactivity measurement of a 0.3 g B^{10} sample in the center of SNEAK as analyzed with the KINEMAT inverse kinetics program, which takes movement of fuel into account (digital plot).

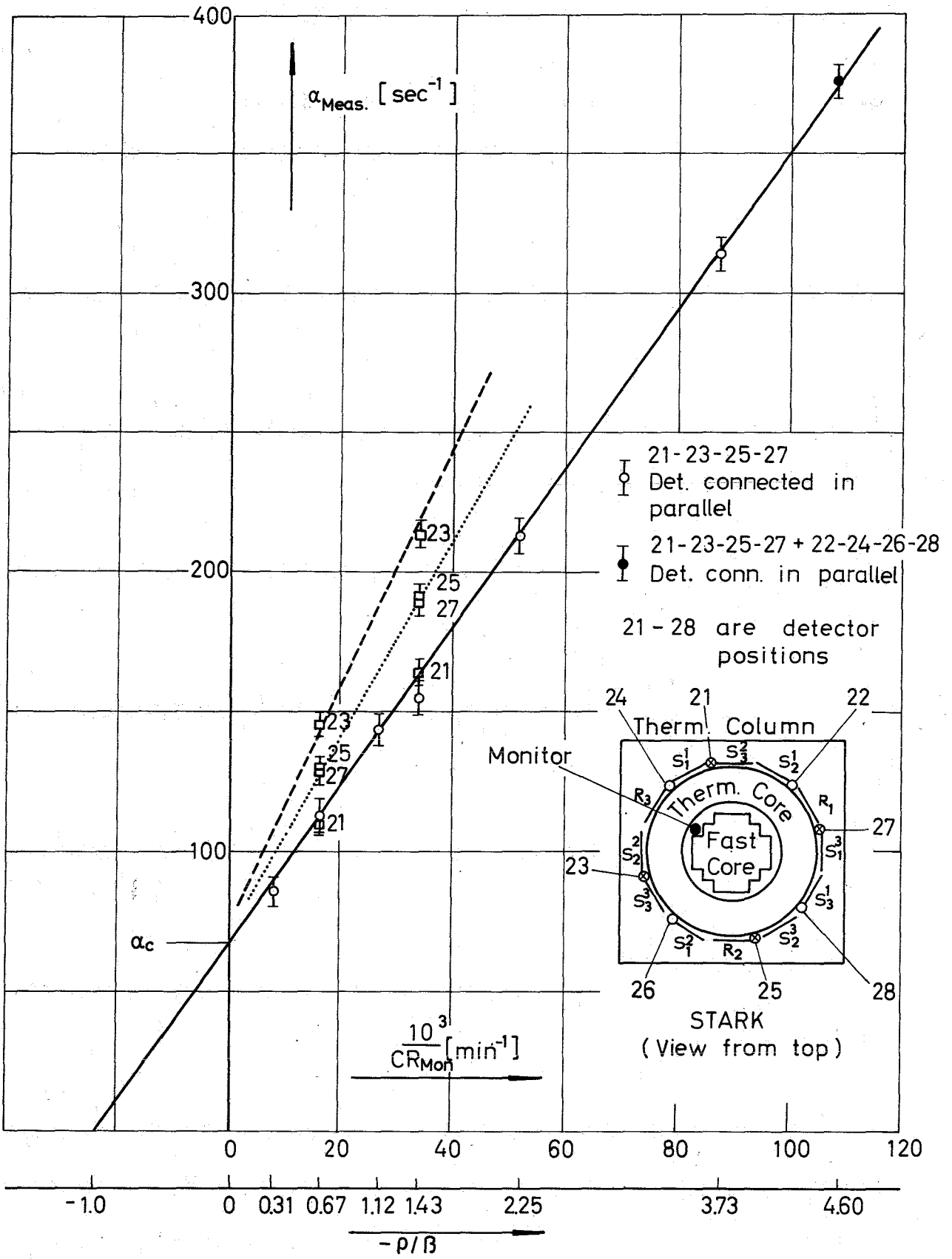

Fig.6 Measured prompt neutron decay constant $\alpha_{Meas.}$ versus reactivity ρ for indicated detector positions